LANGMUIR

pubs.acs.org/Langmuir Article

Self-Aggregation in Aqueous Media of Amphiphilic Diblock and Random Block Copolymers Composed of Monomers with Long Side Chains

Sapir Rappoport, Varvara Chrysostomou, Martha Kafetzi, Stergios Pispas, and Yeshayahu Talmon*

Cite This: *Langmuir* 2023, 39, 3380−3390 Read Online

ACCESS | Metrics & More | Article Recommendations | Supporting Information

ABSTRACT: Amphiphilic diblock copolymers and hydrophobically modified random block copolymers can self-assemble into different structures in a selective solvent. The formed structures depend on the copolymer properties, such as the ratio between the hydrophilic and the hydrophobic segments and their nature. In this work, we characterize by cryogenic transmission electron microscopy (cryo-TEM) and dynamic light scattering (DLS) the amphiphilic copolymers poly(2-dimethylamino ethyl methacrylate)-*b*-poly(lauryl methacrylate) (PDMAEMA-*b*-PLMA) and their quaternized derivatives QPDMAEMA-*b*-PLMA at different ratios between the hydrophilic and the hydrophobic segments. We present the various structures formed by these copolymers, including spherical and cylindrical micelles, as well as unilamellar and multilamellar vesicles.

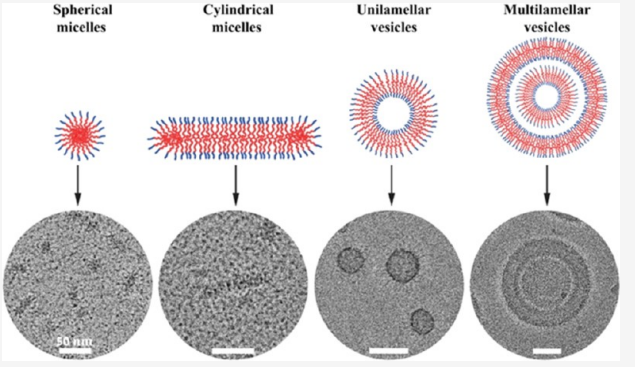

We also examined by these methods the random diblock copolymers poly(2-(dimethylamino) ethyl methacrylate)-*b*-poly(oligo(ethylene glycol) methyl ether methacrylate) (P(DMAEMA-*co*-$Q_{6/12}$DMAEMA)-*b*-POEGMA), which are partially hydrophobically modified by iodohexane (Q_6) or iodododecane (Q_{12}). The polymers with a small POEGMA block did not form any specific nanostructure, while a polymer with a larger POEGMA block formed spherical and cylindrical micelles. This nanostructural characterization could lead to the efficient design and use of these polymers as carriers of hydrophobic or hydrophilic compounds for biomedical applications.

INTRODUCTION

Block copolymers represent a fascinating class of polymeric materials, which have received very widespread attention due to their unique properties and numerous potential applications in the fields of advanced materials (e.g., thermoplastic elastomers), drug and gene delivery, nanomedicine, biomaterials, patterning, porous materials, photoelectric materials, catalysts, etc.[1−3] Block copolymers consist of two or more chemically distinct polymeric segments that are covalently linked together in discrete blocks along the same polymer chain.[1] The combination of the different chemical nature of the block copolymers building blocks, i.e., hydrophilic and hydrophobic character, forms the amphiphilic block copolymers. In particular, amphiphilic block copolymers have been at the focus of extensive scientific interest over the past decades, owing to their ability to self-assemble in bulk, and especially in selective solvents, into a variety of morphologically diverse nanostructures.[2,4] The morphologies include spherical and cylindrical micelles, vesicles, lamellae, bicontinuous structures, and many other complex or hierarchical assemblies.[3−6] A fundamental parameter affecting the morphology of the nanostructures is the molecular architecture of the polymers. The progress in polymer chemistry, polymer synthetic strategies, and polymerization techniques, e.g., living anionic and controlled radical polymerization methods, paved the way to the fabrication of polymers with defined macromolecular architectures, ranging in complexity from linear and cyclic block copolymers to graft or comb-like, miktoarm star, as well as branched and hyperbranched polymers, including dendrimers and bottlebrush polymers.[1,6,7] Among them, bottlebrush copolymers are considered a novel class of block copolymers that have attracted scientific interest. The complexity of their macromolecular architecture leads to their self-assembly in diverse morphological nanostructures.[6]

Inspired by the well-defined macromolecular architecture, shape, and functionality of a complex group of biomolecules known as proteoglycans, a type of bottlebrush-like biopolymers,[8−11] synthetic bottlebrush polymers are a special class of branched or comb/graft polymers consisting of flexible

Received: December 5, 2022
Revised: February 8, 2023
Published: February 21, 2023

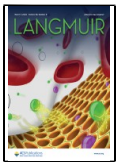

polymeric side chains densely grafted to a linear backbone.[8−12] These structures, also known as molecular brushes or cylindrical polymer brushes, have various architectures depending on the orientation of their backbone and side chains, as well as their grafting densities.[8] The advent of ring-opening metathesis polymerization (ROMP), and particularly controlled/living radical polymerization techniques, including atom transfer radical polymerization (ATRP), reversible addition-fragmentation chain transfer (RAFT), and nitroxide-mediated radical polymerization (NMP), opened to the design of bottlebrush polymers with a great variety of complex structures and well-regulated dimensions.[13−17] According to how the side chains of the bottlebrush polymers are formed, there are three main strategies for the preparation of bottlebrush polymers, the "grafting-through" (polymerization of macromonomers), "grafting-to" (attachment of pre-formed side chains to a backbone), and "grafting-from" (synthesis of side chains from a backbone polyinitiator).[11−13,18−20] Depending on the synthetic route utilized, bottlebrushes polymers with various architectures and topologies can be obtained, including linear, branched, cyclic brushes with block copolymer backbones, random (heterografted) bottlebrush block copolymers, core−shell, brush-on-brush, Janus types, etc.[11,18−21]

The molecular structure and shape of bottlebrushes depend strongly on architectural parameters, namely, the side chain length (i.e., degree of polymerization (DP) of side chain), the backbone length (degree of polymerization of the backbone), the grafting density of the side chains, and the molar masses of the backbone/side chains.[22,23] For example, if the length of the side chains is shorter than that of the backbone, the bottlebrush adopts an extended and wormlike cylindrical shape/conformation. Conversely, molecular brushes with length of side chains similar to or longer than the backbone, adopt spherical shape, which resembles a star-like polymer.[20,23,24] Furthermore, along with the side chain length, the high grafting density of side chains leads to strong steric repulsion between the side chains, causing extension of the backbone. Because of this steric repulsion, the bottlebrushes adopt a wormlike conformation, which promotes the reduction of intermolecular entanglements, resulting in interesting rheological properties, especially in bulk melts.[7,25] Moreover, depending on the size and grafting density of the side chains, the bottlebrush can be physically flexible, semiflexible, or rigid. For instance, the increase in the grafting density of the side chains enhances the stiffness of the bottlebrush polymer.[26] In the case of bottlebrush copolymers, grafting side chains of different lengths in block sequences creates intramolecular spatial asymmetry along the main chain (besides compositional asymmetry), provides complex copolymer architectures, and leads to different nanostructural morphologies and self-assemblies, both in solution and melt, which may have many potential applications in technology and therapeutics.[27,28] Moreover, environmental parameters and external stimuli, like solvent quality, temperature, pH, salt concentration, and light, can strongly affect the bottlebrush polymer conformations, and thus their properties and their potential applications.[8,24] The intriguing properties and behavior of bottlebrush polymers in solid state, melts and solutions, have made them promising candidates for application in diverse areas, ranging from lithography,[29] photonic crystals,[30] supersoft elastomers,[31] in applications such as sensing,[32] aqueous lubrication,[33] antifouling and stimuli-responsive surface coatings,[34] and in areas like nanomedicine,[35] including drug delivery[36,37] and gene/nucleic acid delivery.[38,39]

The particular molecular architectures and tunable structural parameters (e.g., grafting density and length of the backbone and side chains) of bottlebrush polymers provide them with features different from those of linear polymers, which lead to unique self-assembly behavior in solution and bulk.[19] Unlike linear block copolymers, bottlebrush block copolymers with high molar mass and densely grafted architecture do not entangle and can self-assemble, forming structures with large domain sizes up to several hundred nanometers and long-range order. Such a range of domain sizes is desirable for photonic crystal applications.[12,30] Similar to linear block copolymers, bottlebrush block copolymers form micelles in selective solvents (e.g., in aqueous solutions), with resulting micelles larger than those for linear diblock copolymers.[12,40] Furthermore, bottlebrush copolymers present lower critical micelle concentrations (CMCs) than the CMCs of analogous linear block copolymers, probably resulting from their larger size compared with linear copolymers.[40,41] Generally, bottlebrush polymers have been observed to self-assemble into spherical, worm or rodlike, lamellar, and other structures.[19] The nanoscale size of bottlebrushes in solution has allowed them to act as unimolecular micelles that could be used as carriers for small molecules.[20] The unimolecular micelles, i.e., micellar-like core−shell intramolecular assemblies formed by single copolymer chains, of bottlebrushes (e.g., amphiphilic block bottlebrush copolymers) as nanoparticles for drug delivery, present stability and shape control, which is important for drug delivery applications.[42] Another important feature is that molecular bottlebrushes composed of stimuli-responsive segments can be induced to convert their self-assembled conformations from one shape to another by various external stimuli.[19,22,24] For example, molecular bottlebrushes have been shown to exhibit intriguing worm-to-sphere shape transitions in response to external stimuli such as temperature.[43] In conclusion, the tunable structural parameters, architecture, and self-assembly behavior of bottlebrush polymers provide promising potential for producing functional materials with various applications.

Our present report is a morphological study based on cryogenic transmission electronic microscopy (cryo-TEM) imaging of aqueous solutions of the amphiphilic copolymer poly(2-(dimethylamino)ethyl methacrylate)-*block*-poly(lauryl methacrylate) (PDMAEMA-*b*-PLMA) and its quaternized derivatives QPDMAEMA-*b*-PLMA along with the partially hydrophobically modified poly(2-(dimethylamino) ethyl methacrylate)-*b*-poly(oligoethylene glycol methacrylate) random diblock copolymers (P(DMAEMA-co-$Q_{6/12}$ DMAEMA)-*b*-POEGMA) (bottlebrush-type macromolecules). In the former series of amphiphilic copolymers, both hydrophobic and hydrophilic blocks are relatively long chains (compared to the length of the side chain present on each main chain segment), and it is interesting to study how this brush-like chain topology influences the self-assembled structures formed in aqueous media. The latter ones contain relatively long C_6 and C_{12} alkyl chains (i.e., ethylene oligomers) grafted to the polymeric backbone, attached selectively and randomly on a predetermined number of DMAEMA units through quaternization (denoted with the suffix Q_6 and Q_{12}, respectively), with parallel introduction of a positive charge on the respective segments. In other words, the density and hydrophobicity of the brush-like blocks created by the functionalization of

https://doi.org/10.1021/acs.langmuir.2c03294
Langmuir 2023, 39, 3380−3390

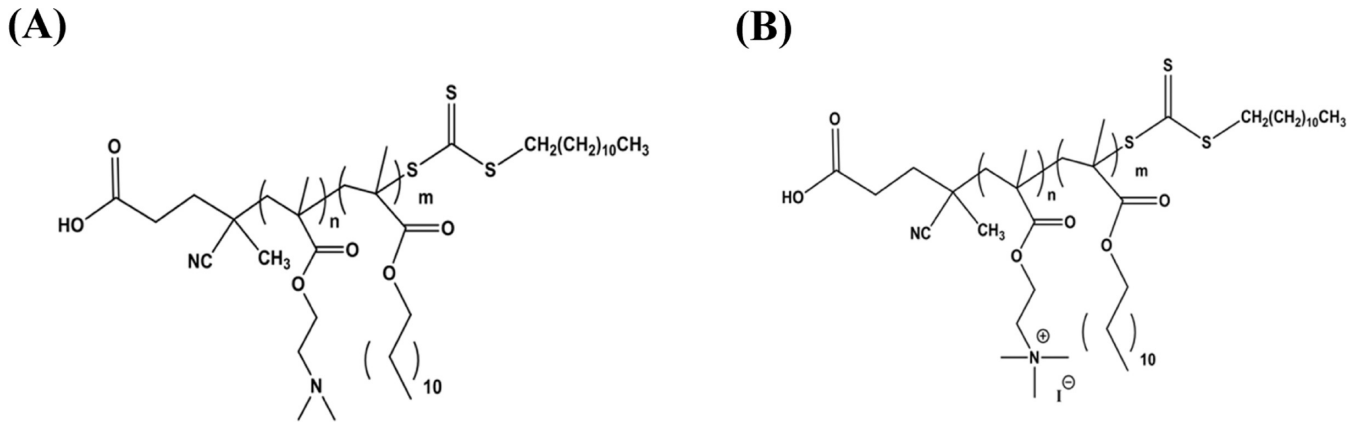

Figure 1. Chemical formulae of (A) PDMAEMA-*b*-PLMA and (B) QPDMAEMA-*b*-PLMA amphiphilic block copolymers.

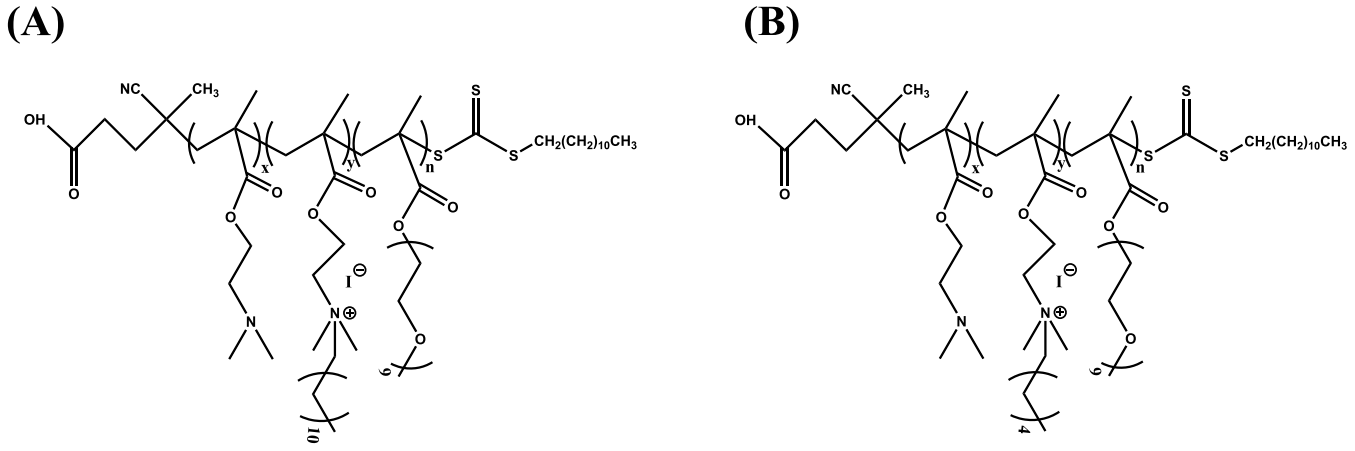

Figure 2. Chemical formulae of P(DMAEMA-*co*-QDMAEMA)-*b*-POEGMA amphiphilic random diblock copolymers, using (A) iodohexane and (B) iodododecane as the quaternization agent.

Table 1. Molecular Characteristics of the Amphiphilic Diblock Copolymers

sample	M_w (×10^4) (g/mol)	M_w/M_n [a]	% wt PDMAEMA [b]	% wt QPDMAEMA [c]	% wt PLMA [b]	quarternization agent
PDMAEMA-*b*-PLMA-1	1.78[a]	1.35	64		36	
PDMAEMA-*b*-PLMA-2	2.16[a]	1.12	18		82	
QPDMAEMA-*b*-PLMA-1	2.80[c]	1.35		77	23	methyl iodide
QPDMAEMA-*b*-PLMA-2	2.51[c]	1.12		30	70	methyl iodide

[a]Determined by SEC. [b]Determined by ^{1}H NMR. [c]Calculated based on 100% quaternization.

PDMAEMA are varied simultaneously. Those changes are expected to influence the self-assembly properties of the copolymers in aqueous media, causing some frustration to the amphiphilic macromolecule.

We used cryogenic transmission electron microscopy (cryo-TEM) to image, in their native vitrified state, the nano-aggregates formed by the block copolymers described above. The microscopy images were compared with results from dynamic light scattering (DLS), an in situ solution characterization technique, but of rather lower structural resolution in terms of picturing morphological characteristics of nano-aggregates.

EXPERIMENTAL SECTION

Materials. All of the amphiphilic copolymers were synthesized in-house by RAFT polymerization. Specifically, the syntheses of the amphiphilic diblock copolymers of PDMAEMA-*b*-PLMA and their quaternized QPDMAEMA-*b*-PLMA polyelectrolytes using methyl iodide, as the quaternization agent, had been reported in our previous work.[44] In this study, we examined by DLS and cryo-TEM the self-assembly and morphological behavior of two PDMAEMA-*b*-PLMA copolymers and two QPDMAEMA-*b*-PLMA polyelectrolyte copolymers. Furthermore, the amphiphilic random diblock copolymers of P(DMAEMA-*co*-QDMAEMA)-*b*-POEGMA and their quaternized analogues, utilizing different quaternization agents have been also reported.[45] In the case of the latter, random diblock copolymers, five P(DMAEMA-*co*-QDMAEMA)-*b*-POEGMA, were investigated in this study by DLS and cryo-TEM, in which two of them had been quaternized using iodohexane (denoted here as P(DMAEMA-*co*-Q_6DMAEMA)-*b*-POEGMA) and the other three were quaternized with iodododecane (denoted here as P(DMAEMA-*co*-Q_{12}DMAEMA)-*b*-POEGMA). The chemical structures of the synthesized amphiphilic diblock and random diblock copolymers are depicted in Figures 1 and 2, respectively. Particularly, PLMA was chosen because of its highly hydrophobic nature, which induces self-assembly in aqueous media, its low T_g, which may enhance the equilibration of the self-organized structures, and the presence of long hydrophobic alkyl side chains (in analogy to the long oligoethylene glycol side chains of the POEGMA hydrophilic block, both blocks

https://doi.org/10.1021/acs.langmuir.2c03294
Langmuir 2023, 39, 3380−3390

Table 2. Characteristics of the Amphiphilic Random Diblock Copolymers[e]

sample	M_w ($\times 10^4$) (g/mol)[a]	M_w/M_n[b]	M_w QPDMAEMA ($\times 10^4$)[c]	% wt PDMAEMA	% wt QPDMAEMA[c]	% wt POEGMA[c]	quarternization agent[d]
P(DMAEMA$_{21}$-*co*-QDMAEMA$_{21}$)-*b*-POEGMA$_{12}$ (4Q$_{12}$)	1.8	1.4	1.0	18	53	29	ID
P(DMAEMA$_{21}$-*co*-QDMAEMA$_{21}$)-*b*-POEGMA$_{12}$ (4Q$_6$)	1.6	1.4	0.75	21	46	33	IH
P(DMAEMA$_{34}$-*co*-QDMAEMA$_8$)-*b*-POEGMA$_{12}$ (3Q$_6$)	1.4	1.4	0.3	39	22	39	IH
P(DMAEMA$_{34}$-*co*-QDMAEMA$_8$)-*b*-POEGMA$_{12}$ (3Q$_{12}$)	1.5	1.4	0.4	36	28	36	ID
P(DMAEMA$_{28}$-*co*-QDMAEMA$_{28}$)-*b*-POEGMA$_{86}$ (2Q$_{12}$)	5.8	1.4	1.3	7	22	71	ID

[a]Calculated utilizing the composition of the quaternized copolymers as determined by ^{1}H NMR and the M_w of the precursor copolymers as determined by SEC. [b]Determined by SEC before the quaternization of the precursor copolymers. [c]Determined by ^{1}H NMR. [d]IH: iodohexane, ID: iodododecane. [e]Note: samples 4Q$_{12}$, 4Q$_6$, 3Q$_6$, and 3Q$_{12}$ derived after the partial quaternization of the PDMAEMA$_{42}$-*b*-POEGMA$_{12}$ copolymer. Sample 2Q$_{12}$ derived after the partial quaternization of PDMAEMA$_{56}$-*b*-POEGMA$_{86}$ copolymer. The subscript of the abbreviated sample name specifies the quaternization agent used for the partial modification of dimethylamino groups of the PDMEMA block.

have a bottlebrush-like structure) that add bulkiness to the polymer chain. The latter structural characteristic may frustrate copolymer organization into nanostructures in aqueous media that may lead to the formation of unexpected block copolymer morphologies. Additionally, we have found that the RAFT polymerization of LMA monomer is highly controllable, which enables the synthesis of well-defined amphiphilic block copolymers. The molecular characteristics of all of the amphiphilic copolymers used in this study, as obtained by size exclusion chromatography (SEC) and ^{1}H nuclear magnetic resonance (^{1}H NMR), are summarized in Table 1 for the amphiphilic block copolymers, and in Table 2 for the random diblock copolymers.

Solution Preparation. To investigate the self-assembly behavior of the amphiphilic copolymers, the solutions were prepared in aqueous media using different preparation protocols, depending on the type and composition in hydrophobic/hydrophilic segments of each copolymer. We used filtered Milli-Q H_2O through 0.45 μm hydrophilic PVDF filters and analytical-grade reagents. All of the solutions were prepared at concentrations of 1.0 mg/mL (~0.1 wt %). Concerning the amphiphilic PDMAEMA-*b*-PLMA copolymers, the preparation procedure includes the dissolution of 10 mg of solid polymer in 1 mL of tetrahydrofuran (THF, 99.9%), which is a common solvent for both blocks. Afterward, the mixture was injected under vigorous stirring into 10 mL of Milli-Q H_2O. Then, the mixture was placed under normal stirring for 5 min to equilibrate. In the next step, the solution was heated at 70 °C for 1 h to evaporate THF. This procedure is described as self-organization precipitation[46] and gave the most consistent and reproducible results in terms of size and size polydispersity, based on initial dynamic light scattering measurements. During heating and evaporation of THF, turbidity and bluish tint of the PDMAEMA-*b*-PLMA solutions were observed, indicating the formation of aggregates. After the evaporation of THF, the solution was left for 30 min to cool down and to equilibrate at room temperature. In the last step, the appropriate amount of Milli-Q H_2O was added to compensate the evaporated H_2O. In the case of amphiphilic QPDMAEMA-*b*-PLMA polyelectrolytes, and specifically the QPDMAEMA-*b*-PLMA-1, the solutions were prepared as follows: 10 mg of solid polymer was dissolved directly in 10 mL of 0.01 M NaCl. The solution of 0.01 M NaCl was prepared in filtered Milli-Q H_2O. The QPDMAEMA-*b*-PLMA-2, due to its higher content in the hydrophobic PLMA segment, was not soluble in 0.01 M NaCl. Hence, the same protocol as with the PDMAEMA-*b*-PLMA copolymers was implemented with 0.01 M NaCl solution used as solvent instead of pure H_2O. Regarding the amphiphilic random diblock P(DMAEMA-*co*-QDMAEMA)-*b*-POEGMA copolymers, for samples P(DMAEMA$_{21}$-*co*-QDMAEMA$_{21}$)-*b*-POEGMA$_{12}$, P(DMAEMA$_{22}$-*co*-QDMAEMA$_{20}$)-*b*-POEGMA$_{12}$, P(DMAEMA$_{34}$-*co*-QDMAEMA$_8$)-*b*-POEGMA$_{12}$, and P(DMAEMA$_{33}$-*co*-QDMAEMA$_9$)-*b*-POEGMA$_{12}$, the following procedure was carried out: 10 mg of solid polymer was dissolved in 1 mL of THF. The mixture was left for 1 h to achieve complete dissolution of the solid, and then it was injected under vigorous stirring into 10 mL of Milli-Q H_2O. The mixtures were heated to 50 °C for 90 min to evaporate THF. When THF was evaporated, Milli-Q H_2O was added to the desired final volume. For sample P(DMAEMA$_{28}$-*co*-QDMAEMA$_{28}$)-*b*-POEGMA$_{86}$, the following preparation protocol was used: 10 mg of solid copolymer was dissolved directly in 10 mL of Milli-Q H_2O. Finally, all of the prepared solutions were left overnight to reach equilibrium. Light scattering and cryo-TEM techniques were implemented the next day.

Cryogenic Transmission Electron Microscopy (Cryo-TEM). All of the polymer solutions were studied by cryogenic transmission electron microscopy (cryo-TEM). The specimens for cryo-TEM were prepared in a controlled environment vitrification system (CEVS) at 25 °C and 100% relative humidity to prevent evaporation from the specimen.[47] A carbon-coated perforated polymer film supported on a 200 mesh TEM grid was plasma-etched in a PELCO EasiGlow glow-discharger (Ted Pella, Inc., Redding, CA) to increase its hydrophilicity before the specimen preparation. Inside the CEVS chamber, the grid was held by tweezers; a drop, approx. 5 μL, of the sample was placed on it; and excess solution was blotted away with a filter paper supported on a metal strip, to form a thin film of the solution, ideally less than 300 nm thick. Then, the specimen was vitrified by plunging it into liquid ethane at its freezing point. The specimen was kept in liquid nitrogen until transfer into the TEM for imaging. The specimens were imaged using Thermo Fisher Scientific FEG-equipped, Talos 200C, 200 kV, high-resolution TEM. To enhance image contrast, we used a Volta "phase-plate" system. Images were collected with a Thermo Fisher Scientific Falcon III direct imaging camera. The solutions of all of the amphiphilic copolymers were examined by cryo-TEM at a concentration of 1.0 mg/mL.[47]

Dynamic Light Scattering (DLS). Dynamic light scattering (DLS) measurements were carried out on an ALV/CGS-3 compact goniometer system (ALV GmbH, Germany), equipped with an ALV-5000/EPP multi-τ digital correlator with 288 channels and an ALV/LSE-5003 light scattering electronics unit for stepper motor drive and limit switch control. A JDS Uniphase 22 mW He−Ne laser at λ = 632.8 nm was utilized as the light source. Toluene was used as the calibration standard solvent. Before measurements, the solutions were filtered through 0.45 mm hydrophilic PVDF Millex syringe filters to eliminate dust particles and large aggregates. The filtered solutions were placed into standard 1 cm width cylindrical quartz cuvettes and were equilibrated for 15 min before DLS measurements. Subsequently, an average of five measurements with a duration of 30 s were conducted in an angular range from 30 to 150°. The autocorrelation functions were analyzed by the cumulants method and the CONTIN software. The presented DLS data and figures correspond to measurements at 90° using CONTIN analysis and a concentration of 1.0 mg/mL. Further supplementary information is given in the Supporting Information.

RESULTS AND DISCUSSION

The copolymers we studied consist of a combination of PDMAEMA, QPDMAEMA, PLMA, and POEGMA blocks. These building blocks give the synthesized copolymers interesting functional features for their use in biomedical applications. Briefly, PDMAEMA is a biocompatible hydro-

https://doi.org/10.1021/acs.langmuir.2c03294
Langmuir 2023, 39, 3380−3390

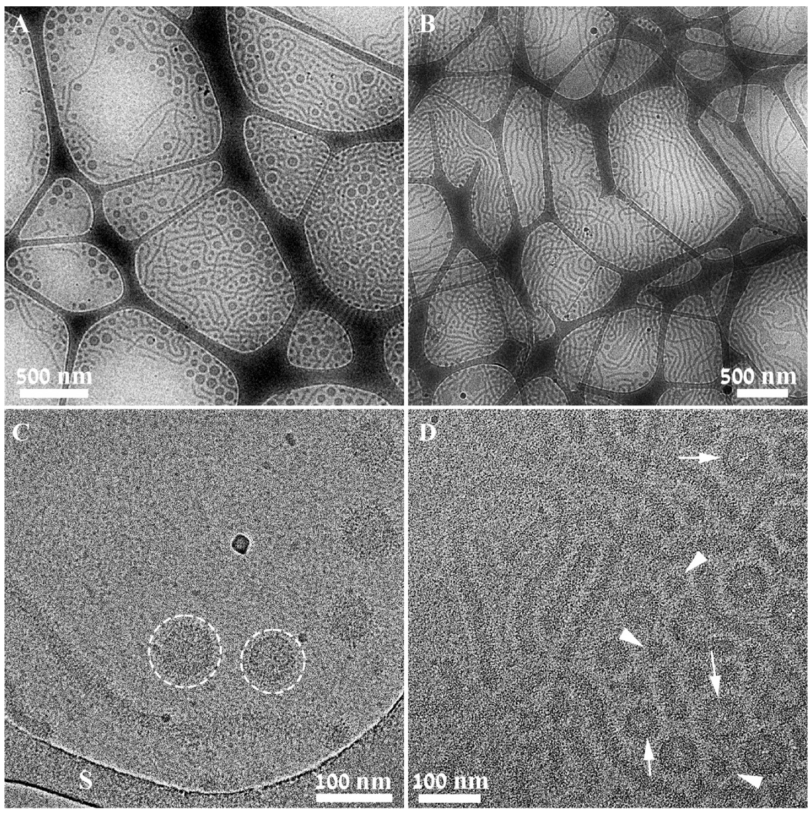

Figure 3. Cryo-TEM images of 1.0 mg/mL PDMAEMA-*b*-PLMA-1 amphiphilic copolymer: spherical, cylindrical, and vesicular structures: (A, B) low magnification; (C, D) high magnification. The corona edges are marked with dashed lines in (C). Arrows in (D) point to vesicles, and arrowheads point to spherical micelles. The support carbon film is the black network seen at low magnification and is denoted by "S" in (C).

philic polymer with stimuli-responsive behavior. External stimuli such as temperature, pH, and ionic strength affect its hydrophilicity. Furthermore, when the tertiary amino group of PDMAEMA is modified to quaternary ammonium salt with a small alkyl iodide (e.g., CH_3I), PDMAEMA is transformed from a weak to a strong QPDMAEMA cationic polyelectrolyte with permanent cationic charge. The positive charge enhances QPDMAEMA hydrophilicity relative to PDMAEMA precursor. Conversely, due to its long alkyl side chains, PLMA exhibits strong hydrophobicity. Moreover, PLMA has a low glass-transition temperature (T_g) of −53 °C, giving the polymer fluidity at room temperature. POEGMA is a brush-like polymer with a hydrophobic backbone and hydrophilic oligoethylene glycol side chains, consisting of nine ethylene glycol units. The hydrophilicity of POEGMA can be changed by modifying the side-chain length, which affects its conformation due to repulsion between the long side chains. Furthermore, POEGMA exhibits biocompatible and stealth properties in in vivo medical applications (analogous to linear poly(ethylene oxide), PEO). In the case of random diblock (P(DMAEMA-*co*-$Q_{6/12}$ DMAEMA)-*b*-POEGMA) copolymers, PDMAEMA blocks are partially quaternized by 1-iodohexane and 1-iodododecane. That way relatively long C_6 and C_{12} alkyl chains are grafted to the polymeric backbone (denoted with the suffix Q_6 and Q_{12}, respectively) with the parallel introduction of a positive charge on the respective chain segments and inducing additional hydrophobic character to the particular blocks and the whole copolymer chain.

Aqueous Solutions of Amphiphilic Diblock Copolymers. The solutions of the amphiphilic diblock copolymers PDMAEMA-*b*-PLMA-1, PDMAEMA-*b*-PLMA-2, and their derivatives QPDMAEMA-*b*-PLMA-1 and QPDMAEMA-*b*-PLMA-2, were imaged by cryo-TEM at a concentration of 1.0 mg/mL. The amphiphilic PDMAEMA-*b*-PLMA-1 copolymer is made of a larger hydrophilic PDMAEMA (M_w = 11,400, 64 wt %) block, and a hydrophobic PLMA (M_w = 6,400, 36 wt %). Cryo-TEM images show that this amphiphilic copolymer forms three coexisting structures in aqueous solution, namely, spherical and cylindrical micelles, as well as vesicular structures also known as "polymersomes" (Figure 3). Figure 3A,B shows low-magnification images of these structures, while Figure 3C,D shows higher-magnification images. The spherical core-corona micelles (arrowheads in Figure 3D) have a core diameter of 20 nm and a corona with a width of 10 nm. The diameters of the core and the corona are the same for the cylindrical ("threadlike" or "wormlike") micelles, whose total length reach several micrometers. One may argue that cylindrical micelles may be a result of spherical micelle secondary assembly. The vesicular structures have the same width of corona, and the width of the hydrophobic layer is 3.5 nm (arrows in Figure 3D). The dimensions determined by cryo-TEM for the compartments of the three types of assembled structures compare rather well with the calculated dimensions of fully extended core and corona individual blocks (Table S1), indicating the actual molecular arrangement and conformational adaptation of copolymer chains into aggregates in each case (since completely extended blocks cannot be found either in the core or the corona domains). Some differences in the core-corona domains dimensions of the compartments of the nanostructures, due to different packing of copolymer chains depending on the particular morphology of aggregates, are expected. In the images, the outer corona is

https://doi.org/10.1021/acs.langmuir.2c03294
Langmuir 2023, 39, 3380−3390

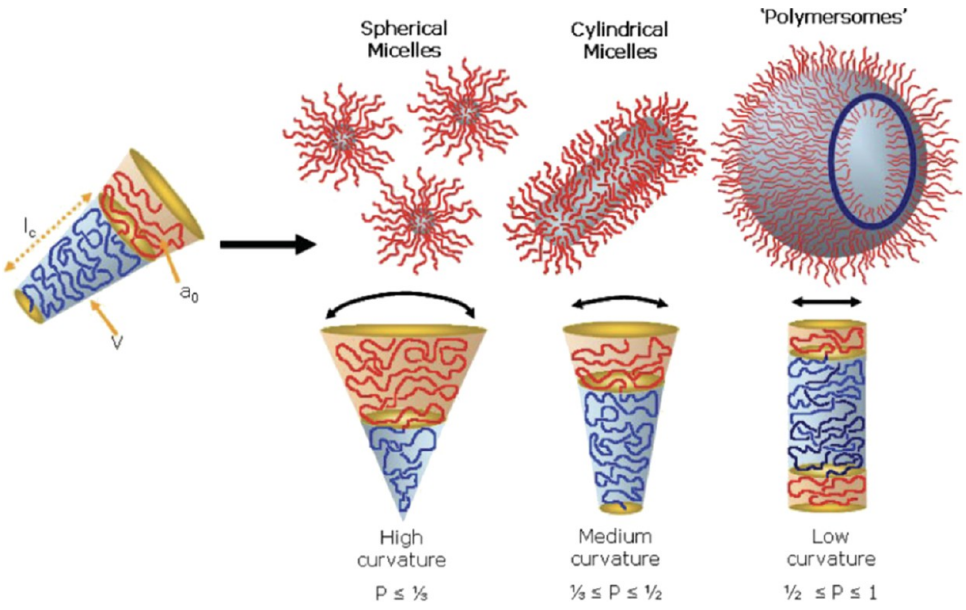

Figure 4. Self-assembled structures of amphiphilic block copolymers in a selective solvent. The polymer curvature determines the formed structure, which can be estimated by calculating the dimensionless packing parameter, $P = v/a_0l_c$.[49] Note that blue refers here to the hydrophobic part, contrary to the commonly used designation. Reproduced with permission from ref 49. Copyright 2009 WILEY-VCH Verlag GmbH & Co. KGaA, Weinheim.

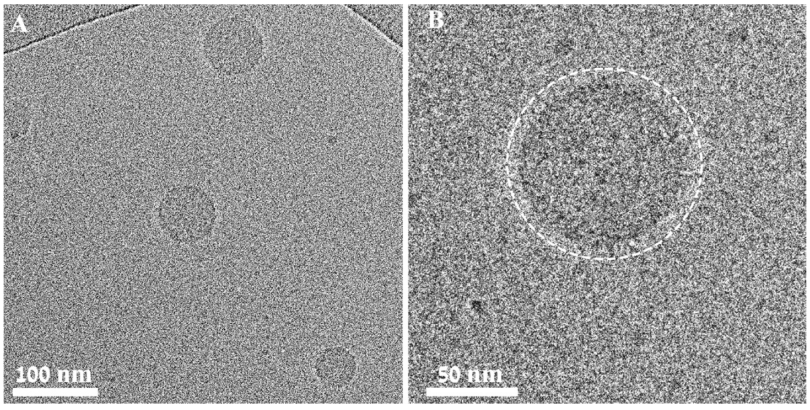

Figure 5. Cryo-TEM images of 1.0 mg/mL PDMAEMA-*b*-PLMA-2 amphiphilic copolymer: (A) vesicular structures with a diameter of 50−90 nm; (B) A higher-magnification image of a vesicular aggregate, showing its 7 nm corona width (lighter halo). The edge of the outer corona is marked with a dashed line.

marked in the dashed line in Figure 3C, but it is difficult to see the inner corona of the vesicle membranes because cryo-TEM images are projections of the structures. The overall size of the vesicles is 60−80 nm. The size range of the vesicles depends largely on the kinetics of membrane size growth.[48] The DLS results indicate aggregates in a range of R_h = 30−900 nm (D_h = 60−1800 nm roughly, Figure S1). It is expected that larger aggregates may be difficult to be detected by DLS due to filtration (fragmentation of wormlike aggregates due to filtration may also take place). The large range of diameters in DLS is a result of multiple types of aggregates in the copolymer solutions (PDI values from DLS are rather high, Table S1). The coexistence of the three structures may be due to polydispersity in the properties of the synthesized copolymer (i.e., molecular weight and composition), which give different packing parameters, and thus different nanostructures (Figure 4). The dimensionless packing parameter defines the inherent molecular curvature of the block copolymer and is defined as: $P = v/a_0l_c$, where v is the volume of the hydrophobic block, a_0 is the cross-sectional area of the hydrophilic group, and l_c is the fully stretched length of the hydrophobic block. In general, amphiphilic block copolymers with high curvature ($P \leq 1/3$) tend to self-assemble into spherical micelles, amphiphilic block copolymers with medium curvature ($1/3 \leq P \leq 1/2$) tend to self-assemble into cylindrical micelles, and amphiphilic block copolymers with low curvature ($1/2 \leq P \leq 1$) tend to self-assemble to "polymersomes".[49] Another scenario related to the coexistence of three types of nanostructures may be the presence of kinetic phenomena during sample solution preparation. In particular, the chains going from the organic solvent well-solvated phase (molecularly dissolved chains in THF) to the aqueous solution phase (a selective solvent that promotes block copolymers self-assembly into aggregates due to PLMA hydrophobicity) do not rearrange completely into equilibrium self-organized structures, due to the large molecular size and the brush-like molecular structure of the copolymers, which retard chain organiza-

https://doi.org/10.1021/acs.langmuir.2c03294
Langmuir 2023, 39, 3380−3390

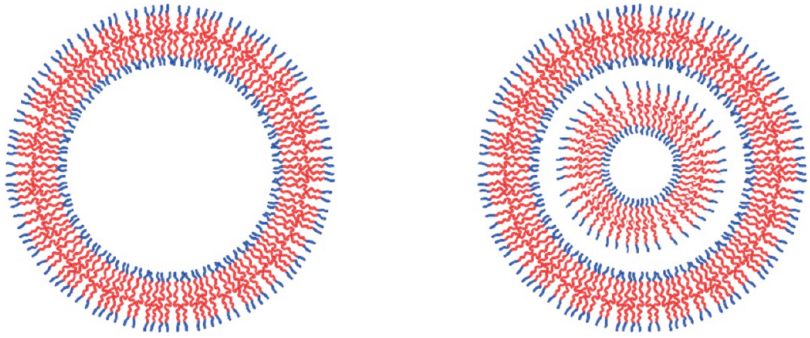

Figure 6. Schematic representation of unilamellar (left) and multilamellar (right) vesicular structures (polymersomes). Red was chosen for the hydrophobic chains, and blue for the hydrophilic ones, as it is usually done in the literature. Colors are inversed in Figure 4, which is reproduced unaltered from ref 49.

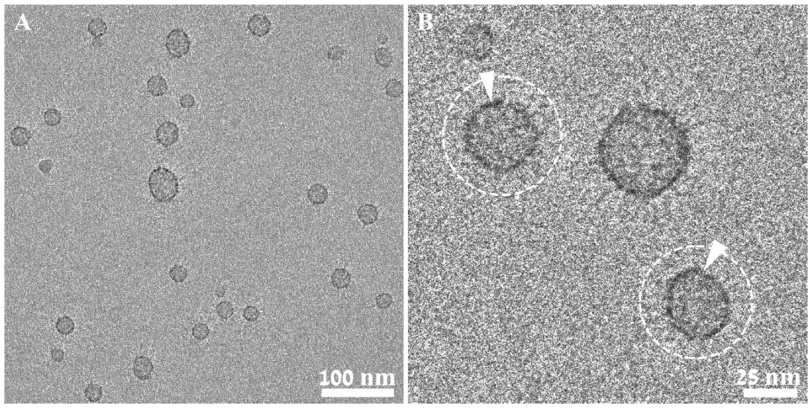

Figure 7. Cryo-TEM images of 1.0 mg/mL QPDMAEMA-*b*-PLMA-1 amphiphilic copolymer shows vesicular aggregates of different sizes. The diameter of the hydrophobic layer is 3.5 nm, and the width of the corona is 10−15 nm. (A) Relatively low-magnification image; (B) higher-magnification image. The outer corona edges are marked with dashed lines in two of the particles, and arrowheads point to the hydrophobic domains.

tion.[2−6] Therefore, copolymer chains are kinetically trapped in assemblies of different morphological characteristics.

In the PDMAEMA-*b*-PLMA-2 amphiphilic copolymer, the hydrophobic PLMA block (M_w = 17,700, 82 wt %) is larger than the hydrophilic PDMAEMA (M_w = 3,900, 18 wt %). Figure 5 shows the morphology imaged by cryo-TEM. Figure 5A shows vesicles of different sizes, 50 to 90 nm. The lighter halo surrounding these structures is the PDMAEMA corona. A schematic representation of a vesicular structure is shown in Figure 6 (left). A higher magnification of a vesicular structure is shown in Figure 5B, where the edge of its corona is indicated with a dashed line. The diameter of this aggregate is 90 nm, while the width of the corona is 7 nm, and the width of the hydrophobic layer is about 5 nm, in general agreement with calculations of extended block length shown in Table S1. In all sizes, the hydrophobic layer and the corona have the same width. Since the hydrophilic segment of this copolymer is smaller compared to PDMAEMA-*b*-PLMA-1, it forms structures with a smaller corona. These results are in partial agreement with the DLS data, showing structures with a hydrodynamic radius between 20 and 120 nm (D_h = 40−240 nm, Figure S2). Some discrepancies in dimensions estimated by the two techniques are expected since cryo-TEM determination of structural dimensions of objects is based on contrast imaging, which makes difficult the observation of the limits of less dense domains, like outer limits of micelle or vesicle coronas, whereas DLS measures the hydrodynamic size of nanoparticulate objects in solutions as equivalents to spheres of similar diffusional characteristics (not taking into account size polydispersity effects and stronger weighting of larger/denser objects in DLS measurements).

The QPDMAEMA-*b*-PLMA-1 quaternized derivative is an amphiphilic diblock copolymer consisting of the strong cationic QPDMAEMA polyelectrolyte in a weight content of 77% (M_w = 21,600) and of the PLMA hydrophobic block with a weight content 23% (M_w = 6,400). The solution of QPDMAEMA-*b*-PLMA-1 copolymer was prepared in 0.01 M NaCl to modulate electrostatic interactions related to the strong polyelectrolyte character of the QPDMAEMA block. The increased ionic strength produces charge screening, affecting QPDMAEMA block solubility and conformation, interactions between copolymer chains, and formation of the copolymer self-assembled nanostructures. Vesicular aggregates of QPDMAEMA-*b*-PLMA-1 are shown in Figure 7. The hydrophobic PLMA forms a dense hydrophobic layer, and the hydrophilic QPDMAEMA forms a corona. In Figure 7B, the vesicular structures are shown at higher magnification. The higher contrast spherical shape is the hydrophobic layer of the vesicles. The outer corona of the vesicles is observed, but with weak contrast against the water. To guide the reader, we added dashed lines in Figure 7B to indicate the corona edges of two vesicles, but the corona is quite clearly seen also in the particle that does not have the added dashed line. The hydrophobic layer shows higher contrast because the hydrophobic segments are condensed to minimize their contact with water. According to cryo-TEM, the overall size of the vesicles is 30−70 nm, the

https://doi.org/10.1021/acs.langmuir.2c03294
Langmuir 2023, 39, 3380−3390

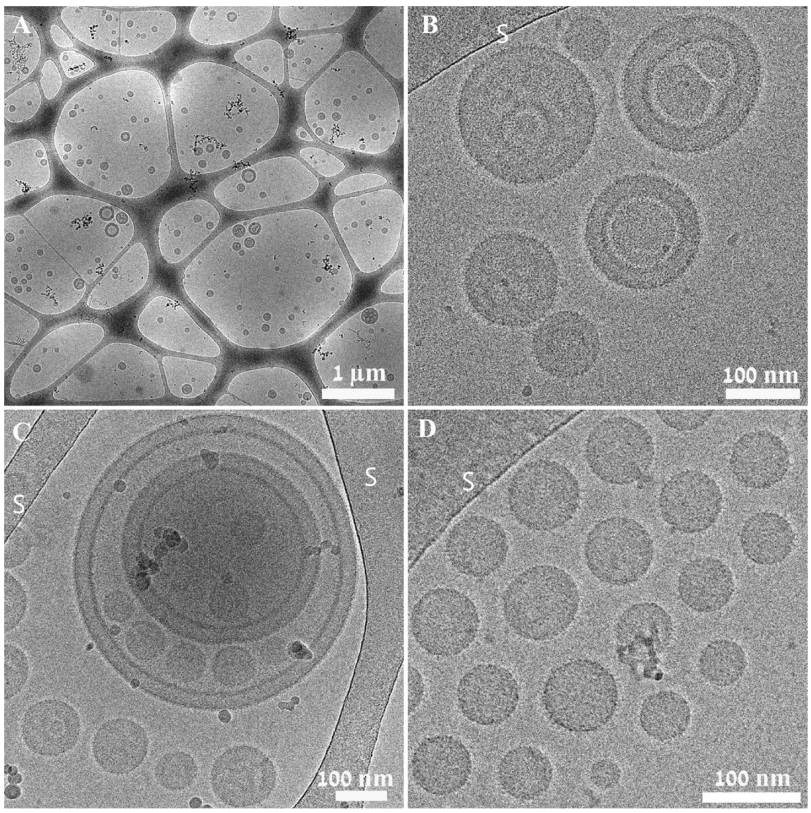

Figure 8. Cryo-TEM images of 1.0 mg/mL QPDMAEMA-*b*-PLMA-2: (A) low-magnification image; (B, C) multilamellar vesicles consisting of several encapsulated unilamellar vesicles; (D) unilamellar vesicles. The support carbon film is the black network seen at low magnification and is denoted by "S" in (B–D).

width of the hydrophobic layer is 3.5 nm, and the width of the corona is 10–15 nm. Such estimates agree with the molecular dimensions presented in Table S1 for each copolymer block. As in PDMAEMA-*b*-PLMA-1, this amphiphilic copolymer has a larger hydrophilic segment, which leads to the formation of vesicles with a large corona. DLS results and specifically CONTIN analysis showed an average diameter of 132 nm.

According to the size distribution (Figure S3), a range of diameters is estimated at 40 nm for small micelles and at 400 nm for larger assemblies (it should be kept in mind that DLS is a low-resolution technique).

Compared to QPDMAEMA-*b*-PLMA-1, the QPDMAEMA-*b*-PLMA-2 polyelectrolyte diblock copolymer is composed of a larger hydrophobic PLMA (M_w = 17,600, 70 wt %) and a smaller QPDMAEMA (M_w = 7,500, 30 wt %). The solution of QPDMAEMA-*b*-PLMA-2 was also prepared and studied in 0.01 M NaCl. In the case of the QPDMAEMA-*b*-PLMA-2 solution, cryo-TEM revealed the formation of different vesicular structures as shown in Figure 8. The overall diameter of these structures is 40–600 nm. The width of the corona, which appears as a bright halo around the aggregates in all of these structures, is estimated at about 10 nm, in rather good agreement with the calculated length of QPDMAEMA blocks in Table S1. The width of the dense hydrophobic layer is 6 nm, and it appears as darkest areas in the images. Unlike the case of copolymer PDMAEMA-*b*-PLMA-2, in addition to the unilamellar vesicles shown in Figure 8D, also aggregates of vesicles were formed. Different structures are shown in Figure 8A at a relatively low magnification, and vesicular aggregates are shown in Figure 8B,C at a higher magnification. These aggregates are multilamellar vesicles, some of which consist of several unilamellar vesicles, with several levels of encapsulation. A schematic representation of unilamellar and multilamellar vesicular structures is shown in Figure 6.

The overall size of the aggregates is 100–600 nm, and the size of the vesicles is 40–60 nm. Thus, these results are in agreement with the DLS results, which showed a hydrodynamic diameter range of 40–400 nm. Specifically, DLS results showed monodisperse self-assembled structures with a mean diameter of 112 nm. However, the size distribution (Figure S4) of hydrodynamic diameters is from 40 to 400 nm, indicating the coexistence of small and larger core-corona nanostructures, as visualized by cryo-TEM. Of course, DLS cannot discriminate the two populations of objects and the inner structures of the assemblies.

P(DMAEMA-*co*-$Q_{6/12}$DMAEMA)-*b*-POEGMA Random Diblock Copolymers. This family of copolymers is composed of hydrophilic POEGMA blocks, carrying grafted oligo(ethylene glycol) chains of nine units on every main chain segment, and partially hydrophobically modified PDMAEMA blocks, randomly grafted with hydrophobic C_6 and C_{12} methylene chains on the nitrogen atom of the dimethylamino side groups. This way short and long grafted hydrophobic groups are introduced to the hydrophilic block via quaternization each time, for comparing the effects of hydrophobic side group length on the self-assemblies formed, if any. The quaternization reaction simultaneously introduces permanent positive charges to the functionalized segments, which contribute to the existing hydrophilic character of the main PDMAEMA chain (and can be utilized, e.g., for complexation with DNA chains or other negatively charged species). Since five samples in total are studied here with different hydro-

https://doi.org/10.1021/acs.langmuir.2c03294
Langmuir 2023, 39, 3380–3390

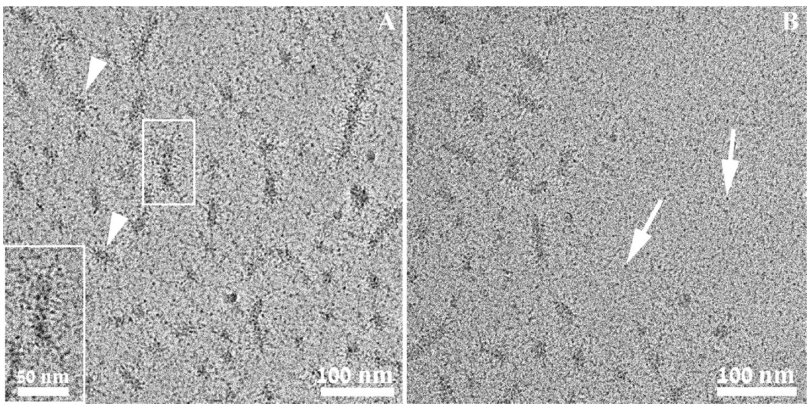

Figure 9. Cryo-TEM images of 1.0 mg/mL $2Q_{12}$: (A) core-corona spherical (arrowheads) and elongated structures, and (B) 6 nm polymer aggregates (arrows). The inset in (A) is a higher-magnification image of the aggregate in the smaller frame, showing the nanostructural details of the aggregate.

phobic side chains and grafting density, for simplicity, we use the notation "mQ_u", where m denotes the code number of the precursor PDMAEMA-*b*-POEGMA diblock copolymer (see Table 2 for the calculated number of each type of segments in the copolymer), together with the degree of quaternization (i.e., 4 for ca. 50% quaternization and 3 for ca. 20% quaternization of the PDMEMA block), and Q_u means that the copolymer is quaternized with iodohexane (Q_6, i.e., C6 side chains) or iodododecane (Q_{12}, i.e., C12 side chains). Therefore, samples $4Q_{12}$ and $4Q_6$ are derived from the same precursor diblock, which has a larger content in PDMAEMA block; they have similar degrees of quaternization (ca. 50% of DMAEMA segments) but different side chains. Similarly, $3Q_6$ and $3Q_{12}$ are obtained from the same diblock precursor as $4Q_{12}$ and $4Q_6$, but the degree of quaternization is lower now (ca. 20% of DMAEMA segments). Sample $2Q_{12}$ is derived from another precursor PDMAEMA-*b*-POEGMA diblock that has a much longer POEGMA block compared to the rest, and a PDMAEMA block of similar length, while the degree of PDMAEMA quaternization is similar to $4Q_{6/12}$ copolymers (ca. 50% of DMAEMA segments). The aqueous solutions of samples $3Q_6$, $3Q_{12}$, and $2Q_{12}$ were investigated by cryo-TEM and DLS at a concentration of 1.0 mg/mL. The DLS size distribution graphs from CONTIN analysis are provided in the Supporting Information as additional evidence.

Based on DLS results and the molecular structure of the random block copolymers, where hydrophobic segments are randomly mixed with hydrophilic ones, large multichain assemblies (probably compound-like micelles[5]) are anticipated for samples $4Q_{12}$, $4Q_6$, $3Q_{12}$, and $3Q_6$ (Figures S5−S8). However, such nanostructures were not recorded by cryo-TEM. According to cryo-TEM, these samples formed various not-well-defined amorphous aggregates. The overall amphiphilic nature and the complexity/randomness of how hydrophilic and hydrophobic segments/side chains are distributed along the main polymer chain of these copolymers most probably do not allow for very well-defined symmetrical structures to form. Figure S9 shows examples of the ill-defined nanoaggregates of these four block copolymers.

However, sample P($DMAEMA_{28}$-*co*-$QDMAEMA_{28}$)-*b*-$POEGMA_{86}$ ($2Q_{12}$) shows some distinctive and more interesting behavior in the series. This amphiphilic random diblock copolymer has higher POEGMA content compared to the rest of the copolymers (samples $4Q_{12}$, $4Q_6$, $3Q_{12}$, and $3Q_6$), and it is hydrophobically modified by iodododecane (a long alkyl side chain that confers substantial hydrophobicity to the copolymer). It was prepared via post-polymerization quaternization reaction of the $PDMAEMA_{56}$-*b*-$POEGMA_{86}$ copolymer. DLS showed the formation of one type of nanoassemblies (within the resolution of the technique a single broad peak is observed by CONTIN analysis, Figure S10) of mean diameter ca. 90 nm (Table S2). The size polydispersity index was found to be rather large, 0.34. The aggregation number was determined as 79 copolymer chains per aggregate (Table S2).

Cryo-TEM images show the coexistence of different nanostructures as shown in Figure 9. Figure 9A shows spherical core-corona structure (arrowheads) with a core diameter of about 20 nm and a corona width of 15 nm. In this image, one can also see elongated core-corona structures with the same corona width as of the spherical structures, but with a diameter of 15 nm and a length of 30−150 nm. Figure 9B shows the same core-corona structure as well as 6 nm globular aggregates (arrows). These small spherical aggregates could be unimers, or they may be the result of the aggregation of only few more intrinsically hydrophobic chains (as a polydispersity in composition within the material is expected). Only one population with broad size distribution was observed by DLS. The high end of the size distribution from DLS coincides with the largest length measured for the elongated structures in cryo-TEM images. Also, in this case, some of these nanoaggregates observed may be nonequilibrium structures.

CONCLUSIONS

We used cryo-TEM and DLS to characterize the size and the morphology of the amphiphilic copolymers PDMAEMA-*b*-PLMA and their quaternized derivatives QPDMAEMA-*b*-PLMA. We also characterized by these methods random diblock copolymers P(DMAEMA-*co*-$Q_{6/12}$DMAEMA)-*b*-POEGMA, which are hydrophobically modified by iodohexane (Q_6) or iodododecane (Q_{12}).

The amphiphilic copolymers PDMAEMA-*b*-PLMA studied differ in the relative size of the hydrophilic and hydrophobic blocks. These copolymers form vesicular structures ("polymersomes"), made of bilayers with the hydrophobic part separated from water by the hydrophilic part, which forms a corona whose width depends on the hydrophilic block size. The copolymer with the larger hydrophilic block also forms spherical and cylindrical micelles, probably as a result of the molecular dispersity of the blocks, leading to different packing

https://doi.org/10.1021/acs.langmuir.2c03294
Langmuir 2023, 39, 3380−3390

parameters of this copolymer. We also imaged the quaternized derivatives QPDMAEMA-*b*-PLMA with different ratios of the hydrophilic/hydrophobic blocks. The quaternized copolymers also form vesicles, but their corona is more extended than that of the vesicles formed from PDMAEMA-*b*-PLMA because of the quaternization and the presence of positive charges of the corona chains. The NaCl solution screens the charges on the copolymers and modulates electrostatic interactions between copolymer chains, enabling them to form vesicles. The QPDMAEMA-*b*-PLMA polymer, with a larger hydrophobic PLMA block, forms multilamellar vesicles in addition to unilamellar ones. These aggregates are probably nonequilibrium structures that are long-lived because of the large molecules of which they are made. Cryo-TEM and DLS results are complementary techniques, except for the filtration of DLS samples that prevent detection of larger aggregates by DLS.

The random diblock copolymers P(DMAEMA-*co*-$Q_{6/12}$DMAEMA)-*b*-POEGMA show different sizes by DLS, but cryo-TEM did not reveal any specific nanostructures for $4Q_{12}$, $4Q_6$, $3Q_6$, and $3Q_{12}$ copolymers. However, $2Q_{12}$ copolymer, which contains a larger content of the hydrophilic POEGMA block, shows coexistence of spherical and elongated core-corona structures, as well as small polymer aggregates.

This systematic nanostructural analysis of a series of block copolymers made of hydrophilic and hydrophobic blocks of different relative block sizes, with and without quaternization, could lead to judicious choice of polymers needed for the formation of desired nanoaggregates to be applied as carriers of various hydrophobic compounds in aqueous media. In principle, the same could be extended to the inverse situation of nanoaggregates in nonaqueous media, where hydrophilic compounds could be dispersed.

■ ASSOCIATED CONTENT

Supporting Information

The Supporting Information is available free of charge at https://pubs.acs.org/doi/10.1021/acs.langmuir.2c03294.

Dynamic light scattering (DLS) data (PDF)

■ AUTHOR INFORMATION

Corresponding Author

Yeshayahu Talmon − *Department of Chemical Engineering and The Russell Berrie Nanotechnology Institute (RBNI), Technion-Israel Institute of Technology, Haifa 3200003, Israel;* orcid.org/0000-0002-9854-3972; Email: ishi@technion.ac.il

Authors

Sapir Rappoport − *Department of Chemical Engineering and The Russell Berrie Nanotechnology Institute (RBNI), Technion-Israel Institute of Technology, Haifa 3200003, Israel*

Varvara Chrysostomou − *Theoretical and Physical Chemistry Institute, National Hellenic Research Foundation, 11635 Athens, Greece*

Martha Kafetzi − *Theoretical and Physical Chemistry Institute, National Hellenic Research Foundation, 11635 Athens, Greece*

Stergios Pispas − *Theoretical and Physical Chemistry Institute, National Hellenic Research Foundation, 11635 Athens, Greece;* orcid.org/0000-0002-5347-7430

Complete contact information is available at: https://pubs.acs.org/10.1021/acs.langmuir.2c03294

Notes

The authors declare no competing financial interest.

■ ACKNOWLEDGMENTS

This work was partially supported by the Israel Science Foundation, Grant#2302/20 (Y.T.). M. K. acknowledges support by the Hellenic Foundation for Research and Innovation (HFRI) under the HFRI PhD Fellowship grant (Fellowship Number: 799). The cryo-TEM work was performed at the Technion Center for Electron Microscopy of Soft Matter.

■ REFERENCES

(1) Feng, H.; Lu, X.; Wang, W.; Kang, N. G.; Mays, J. W. Block Copolymers: Synthesis, Self-Assembly, and Applications. *Polymers* **2017**, *9*, No. 494.

(2) Jiao, W.; Yang, H.; Wu, Z.; Liu, J.; Zhang, W. Self-Assembled Block Polymer Aggregates in Selective Solution: Controllable Morphology Transitions and their Applications in Drug Delivery. *Expert Opin. Drug Delivery* **2020**, *17*, 947−961.

(3) Cabral, H.; Miyata, K.; Osada, K.; Kataoka, K. Block Copolymer Micelles in Nanomedicine Applications. *Chem. Rev.* **2018**, *118*, 6844−6892.

(4) Karayianni, M.; Pispas, S. Self-Assembly of Amphiphilic Block Copolymers in Selective Solvents. In *Fluorescence Studies of Polymer Containing Systems*; Procházka, K., Ed.; Springer: Cham, Switzerland, 2016; Vol. *16*, pp 27−63.

(5) Mai, Y.; Eisenberg, A. Self-Assembly of Block Copolymers. *Chem. Soc. Rev.* **2012**, *41*, 5969−5985.

(6) Karayianni, M.; Pispas, S. Block Copolymer Solution Self-Assembly: Recent Advances, Emerging Trends, and Applications. *J. Polym. Sci.* **2021**, *59*, 1874−1898.

(7) Gadelrab, K. R.; Alexander-Katz, A. Effect of Molecular Architecture on the Self-Assembly of Bottlebrush Copolymers. *J. Phys. Chem. B* **2020**, *124*, 11519−11529.

(8) Mohammadi, E.; Joshi, S. Y.; Deshmukh, S. A. A Review of Computational Studies of Bottlebrush Polymers. *Comput. Mater. Sci.* **2021**, *199*, No. 110720.

(9) Ogbonna, N. D.; Dearman, M.; Cho, C. T.; Bharti, B.; Peters, A. J.; Lawrence, J. Topologically Precise and Discrete Bottlebrush Polymers: Synthesis, Characterization, and Structure−Property Relationships. *JACS Au* **2022**, *2*, 898−905.

(10) Erukhimovich, I.; Theodorakis, P. E.; Paul, W.; Binder, K. Mesophase Formation in Two-Component Cylindrical Bottlebrush Polymers. *J. Chem. Phys.* **2011**, *134*, No. 054906.

(11) Sheiko, S. S.; Sumerlin, B. S.; Matyjaszewski, K. Cylindrical Molecular Brushes: Synthesis, Characterization, and Properties. *Prog. Polym. Sci.* **2008**, *33*, 759−785.

(12) Verduzco, R.; Li, X.; Pesek, S. L.; Stein, G. E. Structure, Function, Self-assembly, and Applications of Bottlebrush Copolymers. *Chem. Soc. Rev.* **2015**, *44*, 2405−2420.

(13) Varlas, S.; Lawrenson, S. B.; Arkinstall, L. A.; O'Reilly, R. K.; Foster, J. C. Self-assembled Nanostructures from Amphiphilic Block Copolymers Prepared via Ring-opening Metathesis Polymerization (ROMP). *Prog. Polym. Sci.* **2020**, *107*, No. 101278.

(14) Matyjaszewski, K. Advanced Materials by Atom Transfer Radical Polymerization. *Adv. Mater.* **2018**, *30*, No. 1706441.

(15) Kerr, A.; Hartlieb, M.; Sanchis, J.; Smith, T.; Perrier, S. Complex Multiblock Bottle-brush Architectures by RAFT Polymerization. *Chem. Commun.* **2017**, *53*, 11901−11904.

(16) Häkkinen, S.; Dyer, B.; Kerr, A.; Perrier, S. Putting the RAFT in GRAFT: Intermolecular Graft Exchange Between Bottlebrush Polymers using Reversible Addition−fragmentation Chain Transfer. *Polym. Chem.* **2022**, *13*, 479−484.

(17) Lamontagne, H. R.; Lessard, B. H. Nitroxide-Mediated Polymerization: A Versatile Tool for the Engineering of Next Generation Materials. *ACS Appl. Polym. Mater.* **2020**, *2*, 5327−5344.
(18) Rzayev, J. Molecular Bottlebrushes: New Opportunities in Nanomaterials Fabrication. *ACS Macro Lett.* **2012**, *1*, 1146−1149.
(19) Li, Z.; Tang, M.; Liang, S.; Zhang, M.; Biesold, G. M.; He, Y.; Hao, S. M.; Choi, W.; Liu, Y.; Peng, J.; Lin, Z. Bottlebrush Polymers: From Controlled Synthesis, Self-Assembly, Properties to Applications. *Prog. Polym. Sci.* **2021**, *116*, No. 101387.
(20) Xie, G.; Martinez, M. R.; Olszewski, M.; Sheiko, S. S.; Matyjaszewski, K. Molecular Bottlebrushes as Novel Materials. *Biomacromolecules* **2019**, *20*, 27−54.
(21) Chen, K.; Hu, X.; Zhu, N.; Guo, K. Design, Synthesis, and Self-Assembly of Janus Bottlebrush Polymers. *Macromol. Rapid Commun.* **2020**, *41*, No. 2070045.
(22) Zhao, B. Shape-changing Bottlebrush Polymers. *J. Phys. Chem. B* **2021**, *125*, 6373−6389.
(23) Kang, J. J.; Shehu, K.; Sachse, C.; Jung, F. A.; Ko, C. H.; Barnsley, L. C.; Jordan, R.; Papadakis, C. M. A Molecular Brush with Thermoresponsive Poly(2-ethyl-2-oxazoline) Side Chains: A Structural Investigation. *Colloid Polym. Sci.* **2021**, *299*, 193−203.
(24) Lee, H.-i.; Pietrasik, J.; Sheiko, S. S.; Matyjaszewski, K. Stimuli-responsive Molecular Brushes. *Prog. Polym. Sci.* **2010**, *35*, 24−44.
(25) Paturej, J.; Sheiko, S. S.; Panyukov, S.; Rubinstein, M. Molecular Structure of Bottlebrush Polymers in Melts. *Sci. Adv.* **2016**, *2*, No. e1601478.
(26) Nian, S.; Fan, Z.; Freychet, G.; Zhernenkov, M.; Redemann, S.; Cai, L. H. Self-Assembly of Flexible Linear−Semiflexible Bottlebrush−Flexible Linear Triblock Copolymers. *Macromolecules* **2021**, *54*, 9361−9371.
(27) Aviv, Y.; Altay, E.; Rzayev, J.; Shenhar, R. Assembly of Bottlebrush Block Copolymers and Nanoparticles in Ultrathin Films: Effect of Substrate−Copolymer Interaction on the Nanocomposite Morphology. *Macromolecules* **2021**, *54*, 6247−6256.
(28) Ahmed, E.; Womble, C. T.; Weck, M. Synthesis and Aqueous Self-Assembly of ABCD Bottlebrush Block Copolymers. *Macromolecules* **2020**, *53*, 9018−9025.
(29) Trefonas, P., III; Thackeray, J. W.; Sun, G.; Cho, S.; Clark, C.; Verkhoturov, S. V.; Eller, M. J.; Li, A.; Pavia-Sanders, A.; Schweikert, E. A.; Wooley, K. L. Bottom-up/top-down, high-resolution, high-throughput lithography using vertically assembled block bottle brush polymers. *J. Micro/Nanolithogr., MEMS, MOEMS* **2013**, *12*, No. 043006.
(30) Liberman-Martin, A. L.; Chu, C. K.; Grubbs, R. H. Application of Bottlebrush Block Copolymers as Photonic Crystals. *Macromol. Rapid Commun.* **2017**, *38*, No. 1700058.
(31) Daniel, W. F. M.; Burdyńska, J.; Vatankhah-Varnoosfaderani, M.; Matyjaszewski, K.; Paturej, J.; Rubinstein, M.; Dobrynin, A. V.; Sheiko, S. S. Solvent-free, Supersoft and Superelastic Bottlebrush Melts and Networks. *Nat. Mater.* **2016**, *15*, 183−189.
(32) Reynolds, V. G.; Mukherjee, S.; Xie, R.; Levi, A. E.; Atassi, A.; Uchiyama, T.; Wang, H.; Chabinyc, M. L.; Bates, C. M. Super-Soft Solvent-Free Bottlebrush Elastomers for Touch Sensing. *Mater. Horiz.* **2020**, *7*, 181−187.
(33) Liu, X.; Claesson, P. M. Bioinspired Bottlebrush Polymers for Aqueous Boundary Lubrication. *Polymers* **2022**, *14*, No. 2724.
(34) Li, X.; Prukop, S. L.; Biswal, S. L.; Verduzco, R. Surface Properties of Bottlebrush Polymer Thin Films. *Macromolecules* **2012**, *45*, 7118−7127.
(35) Müllner, M. Molecular Polymer Brushes in Nanomedicine. *Macromol. Chem. Phys.* **2016**, *217*, 2209−2222.
(36) Raj, W.; Jerczynski, K.; Rahimi, M.; Przekora, A.; Matyjaszewski, K.; Pietrasik, J. Molecular Bottlebrush with pH-responsive Cleavable Bonds as a Unimolecular Vehicle for Anticancer Drug Delivery. *Mater. Sci. Eng.: C* **2021**, *130*, No. 112439.
(37) Ohnsorg, M. L.; Prendergast, P. C.; Robinson, L. L.; Bockman, M. R.; Bates, F. S.; Reineke, T. M. Bottlebrush Polymer Excipients Enhance Drug Solubility: Influence of End-group Hydrophilicity and Thermoresponsiveness. *ACS Macro Lett.* **2021**, *10*, 375−381.
(38) Floyd, T. G.; Song, J. I.; Hapeshi, A.; Laroque, S.; Hartlieb, M.; Perrier, S. (2022). Bottlebrush Copolymers for Gene Delivery: Influence of Architecture, Charge Density, and Backbone Length on Transfection Efficiency. *J. Mater. Chem. B* **2022**, *10*, 3696−3704.
(39) Dalal, R. J.; Kumar, R.; Ohnsorg, M.; Brown, M.; Reineke, T. M. Cationic Bottlebrush Polymers Outperform Linear Polycation Analogues for pDNA Delivery and Gene Expression. *ACS Macro Lett.* **2021**, *10*, 886−893.
(40) Alaboalirat, M.; Qi, L.; Arrington, K. J.; Qian, S.; Keum, J. K.; Mei, H.; Littrell, K. C.; Sumpter, B. G.; Carrillo, J.-M. Y.; Verduzco, R.; Matson, J. B. Amphiphilic Bottlebrush Block Copolymers: Analysis of Aqueous Self-Assembly by Small-Angle Neutron Scattering and Surface Tension Measurements. *Macromolecules* **2019**, *52*, 465−476.
(41) Lyubimov, I.; Wessels, M. G.; Jayaraman, A. Molecular Dynamics Simulation and PRISM Theory Study of Assembly in Solutions of Amphiphilic Bottlebrush Block Copolymers. *Macromolecules* **2018**, *51*, 7586−7599.
(42) Chen, Y.; Zhou, H. B.; Sun, Z. Y.; Li, H. A.; Huang, H. H.; Liu, L. X.; Chen, Y. M. Shell of Amphiphilic Molecular Bottlebrush Matters as Unimolecular Micelle. *Polymer* **2018**, *149*, 316−324.
(43) Henn, D. M.; Holmes, J. A.; Kent, E. W.; Zhao, B. Worm-to Sphere Shape Transition of Thermoresponsive Linear Molecular Bottlebrushes in Moderately Concentrated Aqueous Solution. *J. Phys. Chem. B* **2018**, *122*, 7015−7025.
(44) Chrysostomou, V.; Pispas, S. Stimuli-responsive Amphiphilic PDMAEMA-b-PLMA Copolymers and their Cationic and Zwitterionic Analogs. *J. Polym. Sci., Part A: Polym. Chem.* **2018**, *56*, 598−610.
(45) Kafetzi, M.; Pispas, S. Effects of Hydrophobic Modifications on the Solution Self-Assembly of P(DMAEMA-co-QDMAEMA)-*b*-POEGMA Random Diblock Copolymers. *Polymers* **2021**, *13*, No. 338.
(46) Yabu, H. Creation of Functional and Structured Polymer Particles by Self-organized Precipitation (SORP). *Bull. Chem. Soc. Jpn.* **2012**, *85*, 265−274.
(47) Talmon, Y. The Study of Nanostructured Liquids by Cryogenic-temperature Electron Microscopy−A Status Report. *J. Mol. Liq.* **2015**, *210*, 2−8.
(48) Huang, C.; Quinn, D.; Sadovsky, Y.; Suresh, S.; Hsia, K. J. Formation and Size Distribution of Self-assembled Vesicles. *Proc. Natl. Acad. Sci. U.S.A.* **2017**, *114*, 2910−2915.
(49) Blanazs, A.; Armes, S. P.; Ryan, A. J. Self-Assembled Block Copolymer Aggregates: From Micelles to Vesicles and Their Biological Applications. *Macromol. Rapid Commun.* **2009**, *30*, 267−277.

https://doi.org/10.1021/acs.langmuir.2c03294
Langmuir 2023, 39, 3380−3390